

Sill-Net: Feature Augmentation with Separated Illumination Representation

Haipeng Zhang, *Student Member, IEEE*, Zhong Cao, *Student Member, IEEE*,
Ziang Yan, and Changshui Zhang, *Fellow, IEEE*

Abstract—For visual object recognition tasks, the illumination variations can cause distinct changes in object appearance and thus confuse the deep neural network based recognition models. Especially for some rare illumination conditions, collecting sufficient training samples could be time-consuming and expensive. To solve this problem, in this paper we propose a novel neural network architecture called **Separating-Illumination Network (Sill-Net)**. Sill-Net learns to separate illumination features from images, and then during training we augment training samples with these separated illumination features in the feature space. Experimental results demonstrate that our approach outperforms current state-of-the-art methods in several object classification benchmarks.

Index Terms—Feature augmentation, illumination representation, one/few-shot learning, feature disentanglement, image classification.

1 INTRODUCTION

ALTHOUGH deep neural network based models have achieved remarkable successes in various computer vision tasks [1], [2], [3], [4], vast amounts of annotated training data are usually required for a superior performance in many visual tasks. For the object classification task, the requirement for a large training set could be partially explained by the fact that many latent variables (e.g., positions/postures of the objects, the brightness/contrast of the image, and the illumination conditions) can cause significant changes in the appearance of objects. Although collecting a large training set to cover all possible values of these latent variables could improve the recognition performance, for rare latent values such as extreme illumination conditions it could be prohibitively time-consuming and expensive to collect enough training images.

In this paper we restrict our attention to illumination conditions. For many real-world computer vision applications (e.g., autonomous driving and video surveillance) it is essential to recognize the objects under extreme illumination conditions such as backlighting, overexposure and other complicated cast shadows. Thus, we reckon it is desirable to improve recognition models' generalization ability under different illumination conditions in order to deploy robust models in real-world applications.

We propose a novel neural network architecture named *Separating-Illumination Network (Sill-Net)* to deal with such problems. The key idea of our approach is to separate the illumination features from the semantic features in images, and then augment the separated illumination features onto other training samples (hereinafter we name these samples as "support samples") to construct a more extensive feature set for subsequent training (see Figure 1). Specifically, our approach consists of three steps. In the

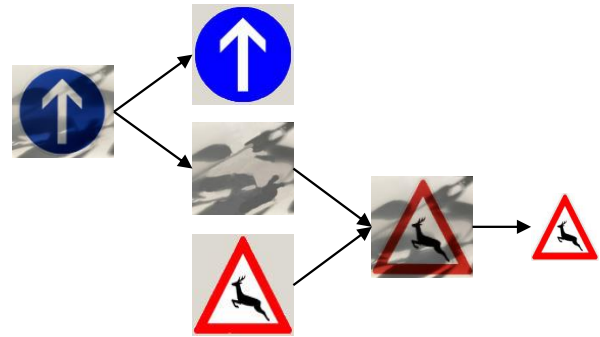


Fig. 1. Illustration of the key idea of our approach. The semantic and illumination representation are separated from the training image (mandatory straight). The illumination representation is used to augment the support sample (deer crossing).

first step, we separate the illumination and semantic features for all images in the existing dataset via a disentanglement method, and use the separated illumination features to build an illumination repository. Then, we transplant the illumination repository to the support samples to construct an augmented training set and use it to train a recognition model. Finally, test images are fed into the trained model for classification. Our proposed approach could improve the robustness to illumination conditions since the support samples used for training are blended with many different illumination features. Thus after training, the obtained model would naturally generalize better under various illumination conditions.

Our contributions are summarized as follows:

1) We develop an algorithm to separate the illumination features from semantic features for natural images. The separated illumination features can be used to construct an illumination feature repository, which can augment the generalized image datasets.

2) We propose an augmentation method to blend support

• H. Zhang, Z. Cao, Z. Yan and C. Zhang are with the Institute for Artificial Intelligence, Tsinghua University (THUAI), Beijing 100084, China, and also with the State Key Laboratory of Intelligence Technologies and Systems, Beijing National Research Center for Information Science and Technologies (BNRist), Department of Automation, Tsinghua University, Beijing 100084, China (e-mail: zhanghp16@mails.tsinghua.edu.cn; caoz10@foxmail.com; yza18@mails.tsinghua.edu.cn; zcs@mail.tsinghua.edu.cn).

• Corresponding Author: H. Zhang and C. Zhang.

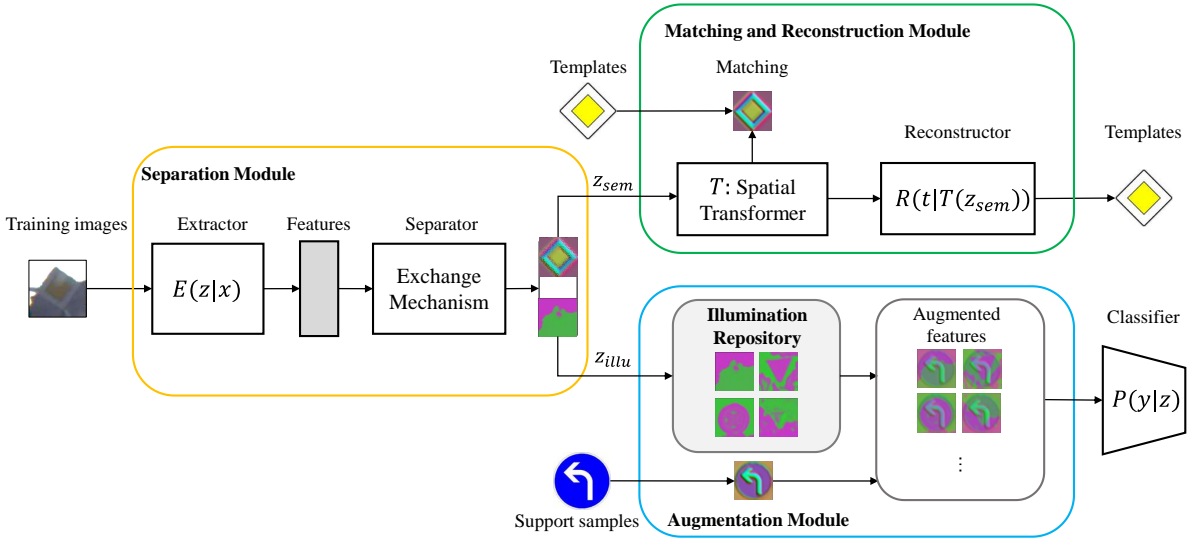


Fig. 2. Illustration of the architecture of Sill-Net. Sill-Net consists of three main modules: the separation module, the matching and reconstruction module, and the augmentation module. The semantic and illumination features are separated by the exchange mechanism in the first module. The semantic features are constrained to be informative by the matching and reconstruction module. The illumination features are stored into a repository. In the augmentation module, we use the illumination features in the repository to augment the support samples (e.g., template images) for training a generalizable model.

samples with the illumination feature repository, which could effortlessly enhance the illumination variety of the training set and thus improve the robustness to illumination conditions of the trained deep model.

3) We evaluate Sill-Net on several object classification benchmarks, i.e., two traffic datasets (GTSRB and TT100K), three logo datasets (Belgalogos, FlickrLogos32, and TopLogo-10) and three generalized one/few-shot benchmarks (*mini*ImageNet, CUB, CIFAR-FS). Sill-Net outperforms the state-of-the-art (SOTA) methods by a large margin in most cases.

2 PROPOSED METHOD

In this section, we introduce our *Separating-Illumination Network* (*Sill-Net*). Sill-Net first learns to separate the semantic and illumination features of training images. Then the illumination features are blended with the semantic feature of each support sample to construct an augmented feature set. Finally, we train again on the illumination-augmented feature set for classification. The architecture of our method is illustrated in Figure 2.

Sill-Net mainly consists of the following modules: the separation module, the matching and reconstruction module, and the augmentation module. In detail, we implement the method in three steps:

1) The separation module is trained to separate the features into semantic parts and illumination parts for all training images. The matching and reconstruction module promotes the learning of better semantic feature representation. The learned illumination features are stored into an illumination repository. The details are illustrated in Section 2.1.

2) The semantic feature of each support image is combined with all illumination features in the repository to build an augmented feature set to train the classifier. The augmentation module is illustrated in Section 2.2.

3) Test images are input into the well-trained model to be predicted in an end-to-end manner, referring to Section 2.4.

This approach assumes that the illumination distribution learned from training data is similar to that of test data. Thus the illumination features can be used as feature augmentation for sufficient training.

We can choose different support samples in different visual tasks. For instance, in conventional classification tasks, we use the real training images as support samples; in one-shot classification tasks, we construct the support set with template images (i.e., graphic symbols visually and abstractly representing semantic information).

2.1 Separate semantic and illumination features

Let $\mathcal{X} = \{(\mathbf{x}_i, y_i, \mathbf{t}_i)\}_{i=1}^N$ represent the labeled dataset of training classes with N images, where \mathbf{x}_i denotes the i -th training image, y_i is the one-hot label, and \mathbf{t}_i denotes the corresponding template image (or any other image of the object without much deformation).

A feature extractor denoted by $E(\mathbf{z}|\mathbf{x})$ learns the separated features \mathbf{z} from images \mathbf{x} , where \mathbf{z} can be split along channels: $\mathbf{z} = [\mathbf{z}_{sem}, \mathbf{z}_{illu}]$. Here, \mathbf{z}_{sem} is called the semantic feature, which represents the consistent information of the same category, while \mathbf{z}_{illu} is called the illumination feature.

Here we specify what illumination represents in our paper. The narrow meaning of illumination is one of the environmental impacts which cause the appearance changes but no label changes. We call the features related to all the environmental impacts but are not category-specific as illumination features. Technically, we divide the object feature into different channels, one half determining the category label defined as the semantic feature, and the other half unrelated to the category label defined as the illumination feature. Thus, the following three conditions should be satisfied:

- 1) The semantic feature is informative to reconstruct the corresponding template image.
- 2) The semantic feature can predict the label while the illumination feature can not.

3) The illumination feature should not contain the semantic information.

To satisfy the above conditions, we build the following modules.

Matching and reconstruction module. We first construct a matching module (as shown in Figure 2) to make the semantic feature informative as required by the first condition. Since we design the extractor without downsampling operations to maintain the spatial information of the object, the semantic feature of one real image should be similar to that of its corresponding template image. However, the real image is usually deformed compared to the regular template image. Therefore, we use a spatial transformer [5] \mathcal{T} to correct the deformation. We constrain the transformed semantic feature $\mathcal{T}(\mathbf{z}_{sem(i)}|\mathbf{x}_i)$ to be consistent with the template feature $\mathbf{z}_{sem(i)}|\mathbf{t}_i$ by the mean square error (MSE), that is:

$$\mathcal{L}_{match} = \frac{1}{N} \sum_{i=1}^N (\mathcal{T}(\mathbf{z}_{sem(i)}|\mathbf{x}_i) - \mathbf{z}_{sem(i)}|\mathbf{t}_i)^2. \quad (1)$$

Besides, we design a reconstructor $R(\mathbf{t}|\mathcal{T}(\mathbf{z}_{sem}))$ (as shown in Figure 2) to retrieve the template image \mathbf{t} from the semantic feature \mathbf{z}_{sem} to ensure that it is informative enough. We constrain the reconstructed template image $\hat{\mathbf{t}}_i$ by binary cross-entropy (BCE) loss:

$$\mathcal{L}_{recon} = \frac{1}{N} \sum_{i=1}^N \sum_{j=1}^{|\mathbf{t}_i|} -t_{ij} \log \hat{t}_{ij} - (1 - t_{ij}) \log (1 - \hat{t}_{ij}), \quad (2)$$

where t_{ij} represents the j -th pixel of the i -th template image \mathbf{t}_i . Since the template images are composed of primary colors within the range of $[0, 1]$, binary cross-entropy (BCE) loss is sufficiently efficient for the retrieval [6]. So far, the semantic feature is constrained to be consistent with the template feature and informative enough to be reconstructed to its template image.

Exchange mechanism. To ensure that the semantic feature can predict the label while the illumination feature can not, we utilize a feature exchange mechanism enlightened by [7] to separate the feature. As shown in Figure 3, the semantic feature $\mathbf{z}_{sem(i)}$ of one image \mathbf{x}_i is blended with the illumination feature $\mathbf{z}_{illu(j)}$ of another image \mathbf{x}_j to form a new one through feature mixup [8]:

$$\mathbf{z} = r\mathbf{z}_{sem(i)} + (1 - r)\mathbf{z}_{illu(j)}, \quad (3)$$

where the proportion $r \in [0, 1]$. As required by the condition, the blended feature \mathbf{z} retains the same label y_i as the semantic feature. Hence through training, the semantic feature would learn information to predict the label while the illumination feature would not.

We implement the exchange process for random pairs of images, building a new exchanged feature set:

$$\mathcal{Z}_{ex} = \{r\mathbf{z}_{sem(i)} + (1 - r)\mathbf{z}_{illu(j)}, y_i \mid i, j = 1, \dots, N\}. \quad (4)$$

The mixed features are then input into a classifier P for label prediction. We denote the distribution of the predicted label y given the mixed feature \mathbf{z} by $P(y|\mathbf{z})$. Then we minimize the cross-entropy loss:

$$\mathcal{L}_{class} = -\frac{1}{N_{ex}} \sum_{i=1}^{N_{ex}} \sum_{c=1}^M y_{ic} \log P(y_{ic}|\mathbf{z}_i \in \mathcal{Z}_{ex}), \quad (5)$$

where $N_{ex} = |\mathcal{Z}_{ex}|$ denotes the number of recombined features in the augmented feature set, M represents the class number of all images for training and test, and y_{ic} is the c -th element of the one-hot label y_i .

The semantic feature retains the information to predict the label after training on the exchanged feature set. Besides, the semantic information in the illumination feature would be reduced, because otherwise, it would impair the prediction when it is blended with the other semantic features.

Constraints on illumination features. As required by the third condition, it is essential to impose additional constraints on illumination features to reduce the semantic information. However, it is difficult to find suitable restrictions since the generally used datasets have no illumination labels.

Enlightened by the disentanglement metric proposed in [9], we design a constraint on illumination features by negative Post Interventional Disagreement (PIDA). Given a subset $\mathcal{X}_c = \{(\mathbf{x}_{ci}, y_c)\}_{i=1}^{N_c}$ including N_c images of the same label y_c , we write the loss as follows:

$$\begin{aligned} \mathcal{L}_{illu} &= -PIDA \\ &= -\sum_{c=1}^M \sum_{i=1}^{N_c} \mathcal{D}(\mathbb{E}(\mathbf{z}_{illu}|\mathbf{x}_{ci}, y_c), \mathbf{z}_{illu}|\mathbf{x}_{ci}, y_c), \end{aligned} \quad (6)$$

here, \mathcal{D} is a proper distance function (e.g., ℓ_2 -norm), $\mathbf{z}_{illu}|\mathbf{x}_{ci}, y_c$ is the illumination feature of image \mathbf{x}_{ci} with the same label y_c , \mathbb{E} is the expectation, and N_c is the number of images in class c .

According to Eq. (6), PIDA quantifies the distances between the illumination feature of each same-labeled image $\mathbf{z}_{illu}|\mathbf{x}_{ci}, y_c$ and their expectation $\mathbb{E}(\mathbf{z}_{illu}|\mathbf{x}_{ci}, y_c)$ when the illumination conditions are changed. In the subset \mathcal{X}_c , the semantic information of each image is similar while the illumination information is different. Suppose an undesirable situation that the illumination features capture much semantic information rather than illumination information. The expectation would strengthen the common semantic component and weaken the distinct illumination components, and thus PIDA would be small. It means that the smaller PIDA is, the more semantic information the illumination feature captures compared to illumination information. By maximizing PIDA (i.e., minimizing \mathcal{L}_{illu}), we can effectively reduce the common semantic information remaining in the illumination features.

In summary, the overall loss function in the training phase can be written as:

$$\mathcal{L} = \mathcal{L}_{match} + \mathcal{L}_{recon} + \mathcal{L}_{class} + \mathcal{L}_{illu}. \quad (7)$$

Through the above training, the model learns to split the features into semantic and illumination features.

2.2 Augment samples by the illumination repository

After the first training step, the illumination feature of each image can be separated. These features are collected to construct an illumination repository, expressed as follows:

$$\mathcal{Z}_{illu} = \{\mathbf{z}_{illu(i)}\}_{i=1}^N. \quad (8)$$

We then use the illumination features to augment the support samples by a multiple of the repository size N . Consider $\mathcal{X}^t = \{(\mathbf{x}_i^t, y_i^t, \mathbf{t}_i^t)\}_{i=1}^{N^t}$ with N^t images of label y^t , here we assume that the template images \mathbf{t}_i^t constitute the support set. We combine all

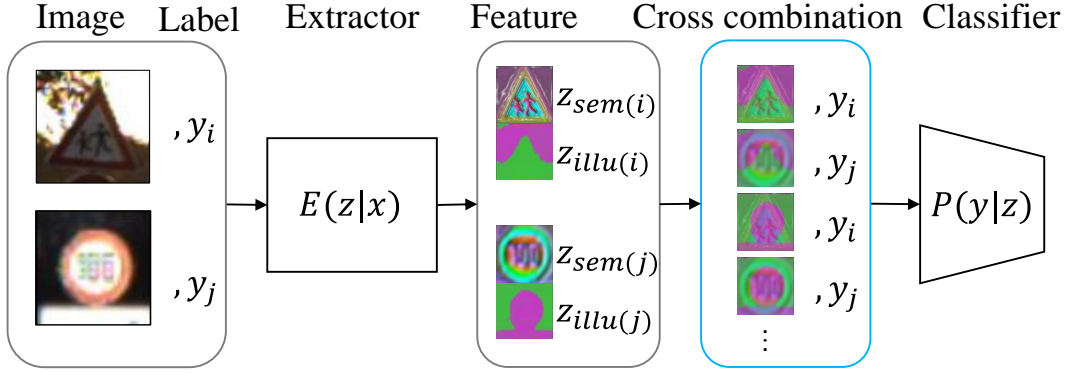


Fig. 3. Illustration of the exchange mechanism. The semantic and illumination features are exchanged between random paired images with labels y_i and y_j . Then we obtain cross combined features labeled the same as the images corresponding to the semantic features. These features are then classified as the specified labels.

illumination features in the repository with the semantic feature of each template $\mathbf{z}_{sem(i)}|_{t_i^t}$ by feature mixup, building an augmented feature set as follows:

$$\mathcal{Z}_{aug} = \{r\mathbf{z}_{sem(i)} + (1-r)\mathbf{z}_{illu(j)}, y_i^t \mid i = 1, \dots, N^t\}, \quad (9)$$

where $\mathbf{z}_{illu(j)} \in \mathcal{Z}_{illu}$.

We train the model again on the feature set \mathcal{Z}_{aug} . So, if a few support samples are provided, the model can be trained on the augmented feature set blended with real illumination features, making it generalizable to test data. The classification loss of augmented training is expressed as follows:

$$\mathcal{L}_{aug} = -\frac{1}{N} \sum_{i=1}^N \sum_{c=1}^M y_{ic} \log P(y_{ic} | \mathbf{z}_i \in \mathcal{Z}_{aug}), \quad (10)$$

where $N = |\mathcal{Z}_{aug}|$ denotes the number of all recombined features in the augmented feature set.

Now, the model has been trained to be generalizable for test.

2.3 Operations on the illumination repository

There are two important factors of the illumination repository: the diversity of illumination characteristics and the size of the repository.

According to the previous analysis, it is important to obtain rich and diverse illumination features. The diversity of the illumination repository determines the final accuracy of image recognition. Here are two ways to obtain a rich and diverse illumination repository. One is to collect large amounts of training images containing rich and diverse illumination characteristics. Another way is to augment the illumination repository during the training phase. Assumed that all the illumination features are from a feature space, so we linearly combine these illumination features to generate new ones. For simplicity, we linearly interpolate random pairs of illumination features to form an expanded repository:

$$\mathcal{Z}_{illu}^{exp} = \{\gamma\mathbf{z}_{illu(i)} + (1-\gamma)\mathbf{z}_{illu(j)} \mid \mathbf{z}_{illu(i)}, \mathbf{z}_{illu(j)} \in \mathcal{Z}_{illu}, \gamma \in [0, 1]\} \quad (11)$$

Besides, the size of the illumination repository directly affects the time cost of the application. When the illumination repository is

very large, the calculation in the training phase is time-consuming. In order to increase the speed of the training phase, reducing the size of the illumination repository is an important method. Compressing the illumination repository is a possible way to reduce the size without decreasing much of the accuracy of image recognition. Some training images are usually obtained under similar illumination conditions, so that some illumination features will be very similar. We can choose some representative illumination features to replace the original illumination features, so that the illumination repository can be compressed. Clustering is a simple and useful method to find representative repository features avoiding much information loss caused by data selection.

Now we have constructed an illumination repository with representative and diverse illumination features via selection and expansion. Our illumination repository is pre-stored and agnostic to the applied datasets of new tasks. Assume that the repository basically covers the illumination distribution, feature augmentation with the repository can facilitate not only symbolic objects recognition but also general few-shot image classification. Experimental details are shown in section 4.5 and 4.7.

2.4 Inference

The feature extractor and classifier have been fully trained after the first two phases. Given the i -th test image, the feature extractor firstly splits the semantic and illumination feature. Subsequently, the features are blended, and then the classifier outputs the category label \hat{c} , formulated as:

$$\hat{c}_i = \arg \max_c P(y_{ic} | \mathbf{z}_i). \quad (12)$$

The inference is achieved in an end-to-end manner.

3 ARCHITECTURE OF THE NETWORKS

In this section, we introduce the architecture and general parameter settings of the model in detail.

Architecture. We construct the extractor by six convolution layers to separate the semantic and illumination features (see the separation module in Figure 2). To maintain the spatial information of the object, we avoid downsizing the features by using one-stride convolution layers without pooling layers for input images scaled

to the size of 64×64 (we can utilize a few pooling layers for higher-resolution input images as long as retaining the spatial information). We set the channel number of the the extractor’s last convolution layer to six. Then we split the output features in half into semantic and illumination parts along with the channels so that both features have three channels. Instance normalization [10] is used to better reserve the semantic information in the features.

The spatial transformer in the matching module (see Figure 2) is built with two convolution layers followed by two fully connected layers, attached to the last convolution layer of the extractor. The reconstructor (see Figure 2) is built with layers of the extractor in an inversed order. But we modified the first layer’s channel number to be three, the same as that of semantic features since only the semantic parts are reconstructed to the template images. We avoid upsampling operations because the features are always maintained at the original input size. For both the extractor and reconstructor, we use leaky ReLU as the activation function except for the last layers. We use the sigmoid function to normalize the output value within the range $[0, 1]$.

The classifiers (see Figure 2 and Figure 3) are built with six convolution layers and three pooling layers to predict the label. Each convolution layer is followed by batch normalization and leaky ReLU. Subsequently, a fully connected layer and a softmax layer are used to output the label. We choose the convolution kernels of size 5×5 and 3×3 throughout the model.

For the exchange mechanism in the separation module, we exchange the semantic and illumination features between random paired images. To simplify the calculation, we use a random template image as one of the paired images. We can combine the semantic and illumination features via mixup or concatenation, as used in [11].

Parameter settings. The networks are trained using the ADAM optimizer with learning rate 10^{-4} , $\beta = (0.9, 0.999)$ and $\epsilon = 10^{-8}$. The mixup proportion r is set to 0.5 for most experiments. Limited by graphics card memory, we choose the mini-batch size of 16, which can be larger if conditions permit.

The matching and reconstruction loss functions are weighted by proportionality coefficients for optimal results. The weighted overall loss function is expressed as follows:

$$\mathcal{L} = \alpha \mathcal{L}_{match} + \theta \mathcal{L}_{recon} + \mathcal{L}_{class} + \mathcal{L}_{illu}. \quad (13)$$

We can choose α and θ in the range of $[10^{-3}, 10^{-1}]$. When they are too large, the model tends to learn false features with values close to zero. While when they are too small, the model is not able to learn informative semantic features. In our method, α is set as 10^{-2} and θ is set as 10^{-1} .

4 EXPERIMENTS

4.1 Datasets and experimental settings

Datasets. We validate the effectiveness of our method on two traffic sign datasets, GTSRB [12] and Tsinghua-Tencent 100K (TT100K) [13], and three logo datasets, BelgaLogos [14], [15], FlickrLogos-32 [16] and TopLogo-10 [17], because these datasets contain different illumination. Table 1 shows the size and number of classes of each dataset (we use the dataset provided in [6]).

GTSRB [12] is the largest traffic sign dataset containing 51,839 images in 43 classes. It is conventionally divided into the training set with 39,209 images and the test set with 12,630 images. It contains illumination variations, complicated cast shadows as well as imbalanced sample distribution.

TT100K [13]. We use the subset of Tsinghua-Tencent 100K (TT100K) provided by [6]. The traffic sign instances were cropped from scenes to build a classification dataset. 36 classes with available template images are selected for the evaluation.

FlickrLogos-32 [16]. We use the subset of FlickrLogos-32 provided by [6]. 3,372 logo instances in 32 classes were cropped from the original images in FlickrLogos-32.

BelgaLogos [14], [15] dataset contains 10,000 images in 37 classes from everyday life. We use the cropped dataset provided by [6], including 9,475 instances. A severe imbalance is observed from 2 samples to 2,242 samples in one class.

TopLogo-10 [17] includes 10 classes of logos from popular cloth, shoes and accessory brands. As processed by [6], the logos instances are cropped using bounding box annotations. The ‘Adidas’ class is separated into the ‘Adidas-logo’ and the ‘Adidas-text’ classes in the experiments.

TABLE 1
Dataset specifications.

Dataset	GTSRB	TT100K	BelgaLogos	FlickrLogos-32	TopLogo-10
Size	51839	11988	9585	3404	848
Classes	43	36	37	32	11

We also evaluate the effectiveness of illumination feature augmentation on standardized one/few-shot image classification datasets: *miniImageNet* [18], CUB [19] and CIFAR-FS [20].

miniImageNet [18] is introduced by Vinyals et al. in [18] for small sample learning research for the first time. It includes 100 classes randomly chosen from ImageNet ILSVRC-2012 challenge [3] with 600 images of size 84×84 pixels per class. It is split into 64 base classes, 16 validation classes and 20 novel classes.

CUB [19] is the most widely-used dataset for fine-grained visual categorization task. It contains 11,788 images of 200 subcategories belonging to birds, 5,994 for training and 5,794 for testing.

CIFAR-FS [20] is randomly sampled from CIFAR-100 [21] by using the same criteria with which *miniImageNet* has been generated. The average inter-class similarity is sufficiently high to represent a challenge for the current state of the art. Besides, the task becomes harder due to the limited original resolution of 32×32 .

Evaluation tasks. Generally, we evaluate our model by the following steps. 1) Utilize the training dataset (or subset) to separate out the illumination features. 2) The support samples are augmented with the illumination features to form an augmented feature set. 3) Train a classifier on the augmented feature set. 4) Prediction on the test dataset.

We validate our model on the following increasingly difficult classification tasks.

1) Traditional classification of GTSRB dataset

GTSRB is the largest traffic sign dataset containing images with various illumination conditions so that we can collect large amounts of high-quality illumination features by the extractor of our model. We split the GTSRB randomly into a training set (39,209 images) and a test set (12,630 images). We train and separate the illumination features on the training set and then augment other training samples with these features. We train another classifier on the augmented features to predict the test samples.

2) One-shot classification on GTSRB and TT100K

In this type of task, the training phase requires no real images of the test classes but one template image for each category. This task is similar to the one-shot classification.

We set up two scenarios for traffic sign classification. In the first scenario, we split GTSRB into a training subset with 22 classes and a test subset with the other 21 classes, where the template images constitute the support set. In the second scenario, we train on GTSRB and test on TT100K for cross-dataset evaluation. We exclude four common classes shared by GTSRB and TT100K in the test set. For convenience, we denote the first scenario by GTSRB→GTSRB and the second by GTSRB→TT100K, where the training set is on the left side of the arrow while the test set is on the right.

For logo classification, we use the largest BelgaLogos as a training set and the remaining two as test sets respectively, denoted by Belga→Flickr32 and Belga→Toplogos. Same as above, we remove four common classes in FlickrLogos-32 and five in Toplogo-10 shared by BelgaLogos.

3) Cross-domain one-shot classification on BelgaLogos, FlickrLogos-32 and TopLogo-10

To further validate the generalization of our method, we perform a cross-domain one-shot evaluation by another two experiments, where the model is trained on traffic sign datasets and tested on logo datasets. Specifically, we train the model on GTSRB and test on FlickrLogos-32 and Toplogo-10. We denote these two scenarios as GTSRB→Flickr32 and GTSRB→Toplogos. The setup is more challenging compared to the previous scenarios, since we train the model in the domain of traffic sign datasets while we test the model in an entirely different domain of logo datasets.

4) Generalized one/few-shot image classification on *miniImageNet*, CUB and CIFAR-FS

Since our method requires template images for the separation of features, the model can not be directly trained on natural image datasets without regular templates such as ImageNet. However, the repository with diverse illumination features separated from GTSRB can facilitate the classification on natural images via proposed illumination feature augmentation. To stress the genericity of the illumination repository, we perform experiments on standardized few-shot classification datasets: *miniImageNet* [18], CUB [19] and CIFAR-FS [20]. The datasets are split into base classes, validation classes and novel classes, following the settings in [22]. We train the backbone of Wide residual networks (WRN) [23] with the pre-trained model provided by [22]. During training on the base classes, we augment the input images with the illumination features through mixup. Here the mixup proportion r is set to 0.1. Once the backbone is trained, we can extract the features of novel classes and then implement Power Transform and Maximum A Posteriori (PT+MAP) proposed by [22]. The results are presented in Section 4.5

Template image processing. Previous studies [24] have shown that basic image processing on template images (as support samples) helps the network’s generalization. In our experiment, we diversify the template images themselves using the following methods: geometric transformations (including translation, rotation and scaling), image enhancement (including brightness, color, contrast and sharpness adjustment), and blur. The template images are diversified and thus allow the model to learn more generalizable features. We observe that basic processing on template images improves model performance.

TABLE 2
Classification accuracy (%) on GTSRB. The results of the SOTA methods are cited from [25], [26]. The best result is marked in blue.

Methods	Accuracy(%)
MCDNN [25]	99.5
CNN with 3 STNs [26]	99.71
Sill-Net	99.68

4.2 Traditional classification of GTSRB

The results of classification on GTSRB are shown in Table 2. We compare our approach Sill-Net with the SOTA methods, i.e., MCDNN [25] and CNN with spatial transformers [26]. Our method achieves a competitive result with the SOTA methods, as shown in the table. The results indicate that Sill-Net is more adept at one-shot classification, and also capable of traditional classification.

4.3 One-shot classification

We compare our method with Siamese networks [27] (SiamNet), Quadruplet networks [28] (QuadNet), Matching networks [18] (MatchNet) and Variational Prototyping-Encoder [6] (VPE) for one-shot classification, reported in Table 3 and 4. We quote accuracies of the compared methods under their optimal settings, that is, VPE is implemented with augmentation and spatial transformer (VPE+aug+stn version), SiamNet and MatchNet is implemented with augmentation, while QuadNet is without augmentation. As shown in the tables, our method outperforms comparative methods in all scenarios.

TABLE 3
One-shot classification accuracy (%) on traffic sign datasets. The best results are marked in blue.

No. support set	GTSRB→GTSRB (22+21)-way	GTSRB→TT100K 36-way
SiamNet [27]	33.62	22.74
QuadNet [28]	45.2	N/A
MatchNet [18]	53.30	58.75
VPE [6]	83.79	71.80
Sill-Net	97.60	95.59
Sill-Net w/o aug	46.25	45.94

In traffic sign classification, Sill-Net outperforms the second best method VPE by a large margin of 13.81% (accuracy improved from 83.79% to 97.60%) and 23.79% (accuracy improved from 71.80% to 95.59%) respectively in two scenarios (see Table 3). It indicates that training on the features augmented by illumination information does help the real-world classification, even though only one template image is provided. It is notable that in the cross-dataset scenario GTSRB→TT100K, Sill-Net achieves a comparable performance to the intra-dataset scenario GTSRB→GTSRB, while VPE performs much worse in the cross-dataset scenario. We surmise it is because VPE learns latent embeddings generalizable to test classes in the same domain (GTSRB), but the generalization might be discounted when the target domain is slightly shifted (from GTSRB to TT100K). It is observed that the illumination conditions in GTSRB are quite similar to that in TT100K, therefore Sill-Net shows better generalization performance by making full use of the illumination information in GTSRB.

TABLE 4

One-shot classification accuracy (%) on logo datasets. The best results are marked in blue.

No. support set	Belga→Flickr32 32-way	Belga→Toplogos 11-way
SiamNet [27]	22.82	30.46
QuadNet [28]	37.72	36.62
MatchNet [18]	40.95	35.24
VPE [6]	53.53	57.75
Sill-Net	65.21	84.43
Sill-Net w/o aug	52.38	47.95

In logo classification, Sill-Net improves the performance by 11.68% (from 53.53% to 65.21%) and 26.68% (from 57.75% to 84.43%) compared to VPE, respectively in two scenarios (see Table 4). The improvement of accuracies in logo classification is not comparable to that in traffic classification, which might be due to the undesirable quality of the training logo dataset. The GTSRB is the largest dataset with various illumination conditions. And the traffic signs are always complete and well localized in the images so that illumination features can be separated more easily. In contrast, the separation is harder for logo dataset due to incomplete logos, color changes, and non-rigid deformation (e.g., logos on the bottles).

We compare our method to the ordinary convolutional model consisting of a feature extractor and a classifier without feature augmentation, denoted as Sill-Net w/o aug (see the last row of Tables 3 and 4). For a fair comparison, the feature extractor and classifier share the same number of convolutional layers with Sill-Net. We train it on a synthetic dataset composed of the template images after basic processing (i.e., geometric transformations, image enhancement, and blur). The number of training samples is set to be the same as other methods. The results are reported as a reference to show how the Sill-Net performs without illumination feature augmentation. The unsatisfactory results show that the illumination feature augmentation does enhance the recognition ability of the model in one-shot classification.

4.4 Cross-domain one-shot classification

Sill-Net achieves the best results among all methods in cross-domain one-shot classification tasks, as shown in Table 5. It outperforms VPE by a large margin of 23.63% (69.75% compared to 46.12%) in GTSRB→Flickr32 and 39.86% (69.46% compared to 29.60%) in GTSRB→Toplogos.

TABLE 5

Cross-domain one-shot classification accuracy (%). The models are trained on the traffic sign dataset (GTSRB) and tested on the logo datasets. The best results are marked in blue.

No. support set	GTSRB→Flickr32 32-way	GTSRB→Toplogos 11-way
QuadNet [28]	28.41	25.38
VPE [6]	46.12	29.60
Sill-Net	69.75	69.46
Sill-Net w/o aug	53.94	47.54

The results illustrate that our method is still generalizable when the domain is transferred from traffic signs to logos. The unsatisfactory results of VPE are predictable. VPE learns a generalizable

similarity embedding space of the semantic information among the same or similar domain (i.e., from traffic signs to traffic signs or from logos to logos). However, the embeddings learned from traffic signs are difficult to generalize to logos. In contrast, our method learns well-separated semantic and illumination representations and augments the illumination features to the template images from novel domains to generalize the model.

4.5 Generalized one/few-shot image classification

TABLE 6

Generalized 1-shot and 5-shot classification accuracy (%) on *miniImageNet*, CUB and CIFAR-FS. Our method is aligned with the pipeline of PT+MAP with the backbone of WRN, trained with the images augmented by the illumination repository. The best results are marked in blue.

Method	Backbone	<i>miniImageNet</i>	
		1-shot	5-shot
BD-CSPN [29]	WRN	70.31 ± 0.93	81.89 ± 0.60
Transfer+SGC [30]	WRN	76.47 ± 0.23	85.23 ± 0.13
TAFSSL [31]	DenseNet121	77.06 ± 0.26	84.99 ± 0.14
DFMN-MCT [32]	ResNet12	78.55 ± 0.86	86.03 ± 0.42
PT+MAP [22]	WRN	82.92 ± 0.26	88.82 ± 0.13
Illu-Aug(ours)	WRN	82.99 ± 0.23	89.14 ± 0.12
Method	Backbone	CUB	
		1-shot	5-shot
BD-CSPN [29]	WRN	87.45	91.74
Transfer+SGC [30]	WRN	88.35 ± 0.19	92.14 ± 0.10
PT+MAP [22]	WRN	91.55 ± 0.19	93.99 ± 0.10
Illu-Aug(ours)	WRN	94.73 ± 0.14	96.28 ± 0.08
Method	Backbone	CIFAR-FS	
		1-shot	5-shot
DSN-MR [33]	ResNet12	78.00 ± 0.90	87.30 ± 0.60
Transfer+SGC [30]	WRN	83.90 ± 0.22	88.76 ± 0.15
PT+MAP [22]	WRN	87.69 ± 0.23	90.68 ± 0.15
Illu-Aug(ours)	WRN	87.73 ± 0.22	91.09 ± 0.15

To stress the genericity of the illumination features extracted from GTSRB, we conduct our method on standardized few-shot classification benchmarks (i.e., *miniImageNet*, CUB and CIFAR-FS) and compare the performance with other state-of-the-art approaches. We augment the training images with the illumination features extracted from GTSRB when training the backbone and implement Power Transformation and Maximum A Posteriori (PT+MAP) proposed by [22]. The results are shown in Table 6 (our method is denoted by Illu-Aug).

As we can see, our method achieves the state-of-the-art performance on all the benchmarks for both 1-shot and 5-shot classification. Generally, our method performs better when the objects are not deformed much compared to the representative template images, so that it achieves most improvements on the CUB dataset. Also, providing more representative template images (i.e., increase the diversity of template images) to be augmented improves the performance. So our method achieves more improvement on 5-shot classification compared to 1-shot classification. Overall, the results demonstrate that the repository with diverse illumination features separated from GTSRB can facilitate the generalized one/few-shot classification on natural images via our proposed illumination feature augmentation.

4.6 Ablation study

In this section, we delve into the contribution of each component of our method. The components under evaluation include the

exchange mechanism, the matching and reconstruction module, the illumination constraint, and template image processing, as shown in Table 7. We disable one component at a time and then record the performance to assess its importance. The experiments are implemented in the one-shot classification scenario GTSRB→GTSRB.

The results demonstrate that the exchange mechanism and matching module are the core components of our method. The accuracy of the model drops to 48.10% without exchange mechanism. It is because that the semantic and illumination features cannot be well separated without the exchange mechanism. The remaining semantic information in the illumination features is useless, or even would interfere with the recognition when they are combined with the semantic features of other objects during feature augmentation, hurting the performance of the model.

Meanwhile, the matching module cooperating with the separation module can further separate the semantic and illumination features. The matching module corrects the deformation of the object features. It retains the concrete semantic information (e.g., the outline of the object and semantic details of the object contents) with the supervision of template images. Without the matching module, the semantic features would not be informative enough, so that the separation module would have difficulty to separate the illumination features from the semantic features. Therefore, the accuracy of the model drops to 54.27% when the matching module is removed.

TABLE 7

Ablation study results (%) in the one-shot classification scenario GTSRB→GTSRB. We disable one component at a time and record the performance of Sill-Net.

Factor	Accuracy (decrement)
w/o exchange mechanism	48.10 (-49.50)
w/o matching module	54.27 (-43.33)
w/o reconstruction module	80.74 (-16.86)
w/o illumination constraint	90.73 (-6.87)
w/o template processing	80.19 (-17.41)
full method	97.60

The accuracy of the model decreases by 16.86% without the reconstruction module. The reconstruction module also strives to make semantic features more informative. The matching module helps the model capture some level of the concrete semantic information, while the reconstruction module prompts to retain more delicate details of the object.

The illumination constraint increases the model performance by 6.87%. Intuitively, the constraint reduces the semantic information in illumination features and thus enhances their quality. Higher-quality illumination representation can improve our feature augmentation method’s effectiveness, which is consistent with the results.

Furthermore, template image processing improves model performance as expected. The processing methods (i.e., geometric transformations, image enhancement, and blur as introduced before) diversify the template images so that the trained model is more generalizable. Under the combined effect of the proposed illumination augmentation in the feature space and the variation of template images, the full model achieves the best results among the existing methods.

4.7 Illumination repository expansion performance

We have constructed a repository containing 51,839 illumination features separated from the training subset of GTSRB. As we observed that the repository includes similar illumination features that might be redundant and less useful for training, we select the representative samples to reduce the number while keeping the important structure of illumination features. Subsequently, we expand the illumination feature space through linear interpolation to further diversify the augmentation features.

Feature selection We first select the illumination features by k -means clustering. The features in the repository are clustered into k partitions. We gather the cluster center of each partition to form a compact repository retaining representative illumination features. In the experiment, we tried both $k = 100$ and $k = 1000$.

Feature interpolation We then expand the feature space using the selected features in the compact repository. We generate new illumination features through linear interpolation of random pairs of the selected features. We evaluate Sill-Net by augmenting the support samples with the generated illumination features in the scenario GTSRB→GTSRB.

TABLE 8

One-shot classification accuracy (%) when augmenting the support samples with generated illumination features from k selected samples in the scenario GTSRB→GTSRB. The best result is marked in blue.

k	Selection	Interpolation
100	85.36	91.12
1000	90.40	97.62

The results are shown in Table 8. As we can see, feature selection can greatly reduce the size of illumination repository (from 51,839 to $k = 100$ or $k = 1000$) while only causes a small decrease in accuracy, indicating that the raw illumination features might be redundant.

Meanwhile, certain expansion of the feature space can generate useful novel illumination features, which can be used as feature augmentation to improve model performance. In our experiment, the linear interpolation method can enhance the accuracy from 85.36% to 91.12% in the case that $k = 100$. When $k = 1000$, the accuracy increases from 90.40% to 97.62%, even outperforms the best result (97.60%, see Table 3) achieved by the raw illumination features.

4.8 Visualization

Feature visualization. Figure 4 shows the separated semantic and illumination features of the images from training and test classes in GTSRB, visualized in the third and fourth lines. Note that the training and test datasets share no common classes. As shown in the figure, the semantic features delicately retain information consistent with the template images for both training and test classes. It is due to three aspects. First, the extractor maintains the size and spatial information of the features. Second, although objects in the input images vary in size and position, the features are corrected to the normal situation corresponding to the template images via the spatial transformer in the matching module. Third, the reconstruction module promotes the semantic feature to retain the details of the objects.

In contrast, the semantic information is effectively reduced in illumination features. These features reflect the illumination

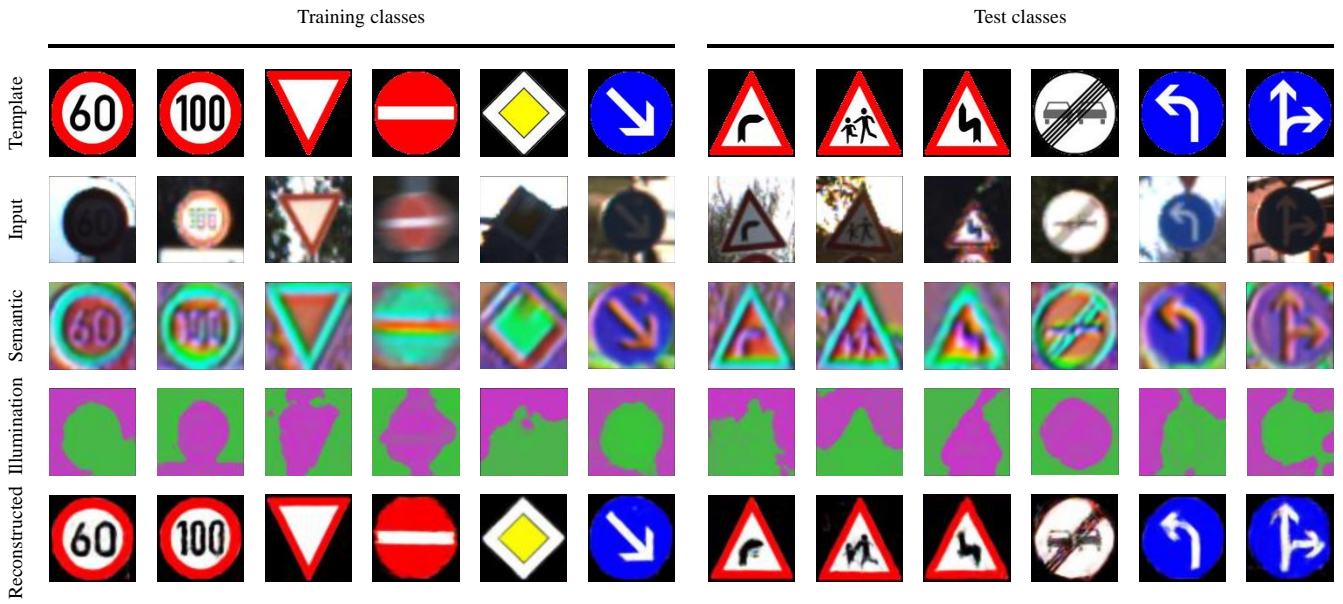


Fig. 4. Visualization of the separated features and the reconstructed template images from training and test classes. The first two rows show the input images and their corresponding template images. The third and fourth rows show the semantic and illumination features of the input images separated by our model. The last row shows the template images reconstructed from the semantic features. Note that the training and test datasets share no common classes.

conditions in the original images to a certain extent. Intuitively, the pink parts in the features represent the bright illumination while the green parts represent the dark illumination. Such well-separated representations lay the foundation for the good performance of our model.

Template reconstruction. While the reconstructor serves to obtain informative semantic features during training, it can also retrieve the template images in the inference phase. As shown in the last row of Figure 4, the reconstructor robustly generates the template images of both the training and test samples, regardless of illumination variance, object deformation, blur, and low resolution of the images. Not only outlines of the symbol contents but also fine-details are well restored in the generated template images, which improves the reconstruction results by VPE. Our results further demonstrate that the proposed model have learned good represents of semantic information for both classification and reconstruction.

Bad cases. Sill-Net fails when the input images suffer fragmentary logos, color changes and non-rigid deformation. The separation of the semantic and illumination features are difficult due to the inconsistency between the templates and input images for these cases. We study the bad cases of the logos, as shown in Figure 5. In the first column, the logo in the image is incomplete. The logo template displays a complete “BASE” while the real image shows only the first letter “B”. The logo in the second column suffers severe color changes. And the remaining logos have various non-rigid deformations, which is difficult for the spatial transformation network (STN) to deal with. The bad quality of logos impairs the representation of semantic features and the reconstruction, resulting in unsatisfactory performance on the logo datasets.

5 DISCUSSIONS

So far, our studies have validated the feasibility and effectiveness of illumination-based feature augmentation. The success of Sill-

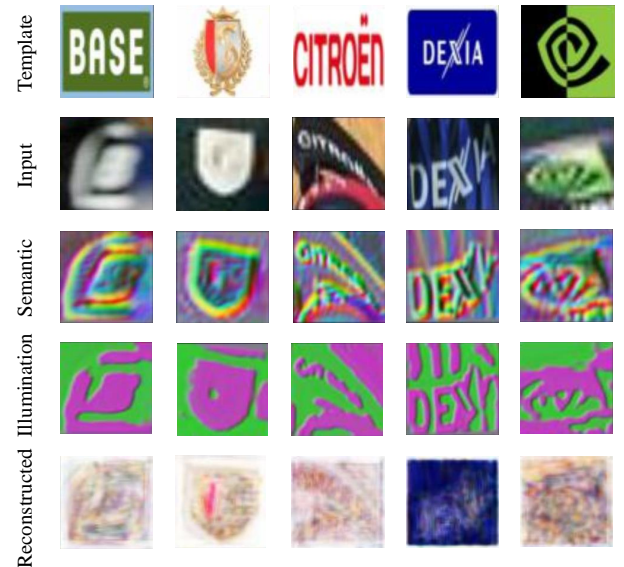


Fig. 5. Bad cases of the logo datasets.

Net benefits from the well-separated illumination features. The idea of learning good semantic and illumination features before training a classifier is consistent with the thinking of decoupling representation and classifier [34]. Compared to the existing approaches [6], [28], our method not only achieves the best results on the traffic sign and logo classifications, but also learns intuitively interpretable semantic and illumination representation and performs

better reconstructions.

Our method can be widely applied to a series of training scenarios. In the case that the training samples with certain illumination conditions are limited in the dataset, we can augment these samples with that type of illumination features separated from other images (or simply use the illumination features in our repository). Besides, we can utilize the method to expand a few support samples or even only one (e.g., template images) to form a large training dataset, solving the problem of lacking annotated real data. Overall, the imbalance both in size and illumination conditions of the dataset could be alleviated since we can transplant illumination information to specific training samples with a limited number and illumination diversity.

Here is one question that why we do not classify a test sample by its semantic feature after the separation. Actually, we have to train the classifier with the augmented samples because generally there are not many support samples in few-shot or one-shot scenarios. If we trained the classifier with a few support samples, it would be poor in generalization due to the memorization of deep networks [35]. While when we extend the volume and diversity of the feature set by illumination augmentation, the trained model can be more generalizable.

Our work can be improved from the following aspects.

First, it should be noted that the illumination features learned by our model seem to reflect relative illumination intensity rather than fine details, limited by the lack of illumination supervision. The constraint used in our method improves the quality of illumination features to some extent and thus enhances the model performance. However, other approaches with more stringent constraints or pretraining on illumination supervised data, can be applied to obtain refined illumination representation.

Second, alternative disentanglement methods can be utilized to separate the semantic and illumination features. One of the key challenges we face is the separation of non-semantic features when we only have semantic labels. Although the exchange mechanism does prompt the separation of semantic and illumination information in the split features, we have to apply additional modules or constraints (i.e., matching and reconstruction modules and PIDA) to refine the details. More sophisticated methods need to be proposed to learn better disentangled representations in the weakly-supervised settings.

Third, the spatial transformation network (STN) can be substituted by other networks in the matching module. In traffic sign classifications, STN can well correct the semantic features to be consistent with that of the templates. However, it is sometimes difficult to deal with the non-rigid deformation in logo datasets. Furthermore, general objects might be distinct with the templates in many aspects, such as color variation and changes in visual angles. Two ways can be considered. First, we can choose several different template images for different types of variation. Second, we can develop general networks to deal with such transformations. For instance, we can translating the objects along many such directions (e.g., color and visual angles) in the feature space to the templates via semantic transformations [36].

6 RELATED WORKS

6.1 Data augmentation

Deep learning is always heavily reliant on large amounts of data to avoid the overfitting of the networks. Data augmentation is an effective data-space solution to the problem of limited data [37].

It includes a series of methods that artificially inflate the size of the training dataset through either data warping or oversampling. Augmentations based on data warping transform existing images by some methods while preserving the original labels. These augmentations encompass basic image manipulations such as geometric transformations [38], color space transformations [39], and noise injection [40], as well as deep learning approaches such as adversarial training [41] and neural style transfer [42]. Oversampling augmentations enhance the datasets by generating synthetic training samples. These augmentations can also be divided into basic image manipulations such as image mixing [43], and deep learning approaches including feature space augmentations [44] and GAN-based data augmentations [45].

In this work, we propose a method of feature space augmentation. This kind of augmentations implement the transformation in a learned feature space rather than the input space. DeVries and Taylor [44] discuss the common forms of transformation by adding noise, interpolating, and extrapolating, which opens up further studies into feature space augmentations. Feature space augmentations can be flexibly implemented. It can be applied to auto-encoders in the case that reconstruction back to the input space is necessary [37]. It is also possible to do augmentations in the vector representations from a convolutional neural networks. One of the limitations of feature space augmentation is that the augmented vector representations are difficult to interpret. However, the illumination features we used for augmentation have a clear meaning.

6.2 Feature disentanglement

One important problem of computer vision is to learn the disentangled representation comprising a number of latent factors, with each factor controlling an interpretable aspect of the generated data [46]. Some works focus on disentanglement learning with respect to specified labels [47], [48], [49], [50], [51]. They are proposed to extract features that are composed of two parts: one part summarizes the specified factors of variation associated with the labels (content), while the other summarizes the remaining unspecified variability (style). The concepts of content and style are corresponding to the semantic and illumination parts in this article, respectively. One basic idea is to pair the content factor of a data sample with the style factor of another sample with the same label [47]. The resulting representation should be able to recover the latter sample using a decoder. Such an idea is also applied to a weakly-supervised setting that only members of a given group share the same label are available, whereas different groups are not required to represent different classes [49], [50], [51].

6.3 Few shot learning

Compared to the common machine learning paradigm that involves large-scale labeled training data, the development of Few Shot Learning (FSL) is relatively tardy due to its intrinsic difficulty. Early efforts for FSL were based on generative models that sought to build the Bayesian probabilistic framework [52], [53]. Recently, more attention was paid on meta-learning, which can be generally summarized into five sub-categories: *learn-to-measure* (e.g., MatchNets [18], ProtoNets [54], RelationNets [55]), *learn-to-finetune* (e.g., Meta-Learner LSTM [56], MAML [57]), *learn-to-remember* (e.g., MANN [58], SNAIL [59]), *learn-to-adjust* (e.g., MetaNets [60], CSN [61]) and *learn-to-parameterize* (e.g., DynamicNets [62], Acts2Params [63]). In this work, we used

tasks similar to one-shot learning to evaluate our method. And our methods are basically a data augmentation strategy to solve these data scarcity problems.

7 CONCLUSION

In this paper, we develop a novel neural network architecture named **Separating-Illumination Network (Sill-Net)**. The illumination features can be well separated from training images by Sill-Net. These features can be used to augment the support samples. Our method outperforms the state-of-the-art (SOTA) methods by a large margin in several benchmarks. In addition to these improvements in visual applications, the results demonstrate the feasibility of the illumination-based augmentation method in the feature space in object recognition, which is a potential research direction about data augmentation.

ACKNOWLEDGMENTS

None.

REFERENCES

- [1] A. Krizhevsky, I. Sutskever, and G. E. Hinton, "Imagenet classification with deep convolutional neural networks," *Communications of the ACM*, vol. 60, no. 6, pp. 84–90, 2017.
- [2] K. Simonyan and A. Zisserman, "Very deep convolutional networks for large-scale image recognition," *arXiv preprint arXiv:1409.1556*, 2014.
- [3] O. Russakovsky, J. Deng, H. Su, J. Krause, S. Satheesh, S. Ma, Z. Huang, A. Karpathy, A. Khosla, M. Bernstein *et al.*, "Imagenet large scale visual recognition challenge," *International journal of computer vision*, vol. 115, no. 3, pp. 211–252, 2015.
- [4] K. He, X. Zhang, S. Ren, and J. Sun, "Deep residual learning for image recognition," in *Proceedings of the IEEE conference on computer vision and pattern recognition*, 2016, pp. 770–778.
- [5] M. Jaderberg, K. Simonyan, A. Zisserman *et al.*, "Spatial transformer networks," in *Advances in neural information processing systems*, 2015, pp. 2017–2025.
- [6] J. Kim, T.-H. Oh, S. Lee, F. Pan, and I. S. Kweon, "Variational prototyping-encoder: One-shot learning with prototypical images," in *Proceedings of the IEEE Conference on Computer Vision and Pattern Recognition*, 2019, pp. 9462–9470.
- [7] T. Xiao, J. Hong, and J. Ma, "Elegant: Exchanging latent encodings with gan for transferring multiple face attributes," in *Proceedings of the European conference on computer vision (ECCV)*, 2018, pp. 168–184.
- [8] H. Zhang, M. Cisse, Y. N. Dauphin, and D. Lopez-Paz, "mixup: Beyond empirical risk minimization," *arXiv preprint arXiv:1710.09412*, 2017.
- [9] R. Suter, D. Miladinovic, B. Schölkopf, and S. Bauer, "Robustly disentangled causal mechanisms: Validating deep representations for interventional robustness," in *International Conference on Machine Learning*. PMLR, 2019, pp. 6056–6065.
- [10] D. Ulyanov, A. Vedaldi, and V. Lempitsky, "Instance normalization: The missing ingredient for fast stylization," *arXiv preprint arXiv:1607.08022*, 2016.
- [11] H. Bai, R. Sun, L. Hong, F. Zhou, N. Ye, H.-J. Ye, S.-H. G. Chan, and Z. Li, "Decaug: Out-of-distribution generalization via decomposed feature representation and semantic augmentation," *arXiv preprint arXiv:2012.09382*, 2020.
- [12] J. Stallkamp, M. Schlipsing, J. Salmen, and C. Igel, "Man vs. computer: Benchmarking machine learning algorithms for traffic sign recognition," *Neural networks*, vol. 32, pp. 323–332, 2012.
- [13] Z. Zhu, D. Liang, S. Zhang, X. Huang, B. Li, and S. Hu, "Traffic-sign detection and classification in the wild," in *Proceedings of the IEEE conference on computer vision and pattern recognition*, 2016, pp. 2110–2118.
- [14] A. Joly and O. Buisson, "Logo retrieval with a contrario visual query expansion," in *Proceedings of the 17th ACM international conference on Multimedia*, 2009, pp. 581–584.
- [15] P. Letessier, O. Buisson, and A. Joly, "Scalable mining of small visual objects," in *Proceedings of the 20th ACM international conference on Multimedia*, 2012, pp. 599–608.
- [16] S. Romberg, L. G. Pueyo, R. Lienhart, and R. Van Zwol, "Scalable logo recognition in real-world images," in *Proceedings of the 1st ACM International Conference on Multimedia Retrieval*, 2011, pp. 1–8.
- [17] H. Su, X. Zhu, and S. Gong, "Deep learning logo detection with data expansion by synthesising context," in *2017 IEEE winter conference on applications of computer vision (WACV)*. IEEE, 2017, pp. 530–539.
- [18] O. Vinyals, C. Blundell, T. Lillicrap, D. Wierstra *et al.*, "Matching networks for one shot learning," in *NIPS*, 2016.
- [19] C. Wah, S. Branson, P. Welinder, P. Perona, and S. Belongie, "The caltech-ucsd birds-200-2011 dataset," 2011.
- [20] L. Bertinetto, J. F. Henriques, P. H. Torr, and A. Vedaldi, "Meta-learning with differentiable closed-form solvers," *arXiv preprint arXiv:1805.08136*, 2018.
- [21] A. Krizhevsky, G. Hinton *et al.*, "Learning multiple layers of features from tiny images," 2009.
- [22] Y. Hu, V. Gripon, and S. Pateux, "Leveraging the feature distribution in transfer-based few-shot learning," *arXiv preprint arXiv:2006.03806*, 2020.
- [23] S. Zagoruyko and N. Komodakis, "Wide residual networks," *arXiv preprint arXiv:1605.07146*, 2016.
- [24] L. Tabelini, R. Berriel, T. M. Paixão, A. F. De Souza, C. Badue, N. Sebe, and T. Oliveira-Santos, "Deep traffic sign detection and recognition without target domain real images," *arXiv preprint arXiv:2008.00962*, 2020.
- [25] D. Ciregan, U. Meier, and J. Schmidhuber, "Multi-column deep neural networks for image classification," in *2012 IEEE conference on computer vision and pattern recognition*. IEEE, 2012, pp. 3642–3649.
- [26] A. Arcos-Garcia, J. A. Alvarez-Garcia, and L. M. Soria-Morillo, "Deep neural network for traffic sign recognition systems: An analysis of spatial transformers and stochastic optimisation methods," *Neural Networks*, vol. 99, pp. 158–165, 2018.
- [27] G. Koch, R. Zemel, and R. Salakhutdinov, "Siamese neural networks for one-shot image recognition," in *ICML deep learning workshop*, vol. 2. Lille, 2015.
- [28] J. Kim, S. Lee, T.-H. Oh, and I. S. Kweon, "Co-domain embedding using deep quadruplet networks for unseen traffic sign recognition," *arXiv preprint arXiv:1712.01907*, 2017.
- [29] J. Liu, L. Song, and Y. Qin, "Prototype rectification for few-shot learning," *arXiv preprint arXiv:1911.10713*, 2019.
- [30] Y. Hu, V. Gripon, and S. Pateux, "Exploiting unsupervised inputs for accurate few-shot classification," *arXiv preprint arXiv:2001.09849*, 2020.
- [31] M. Lichtenstein, P. Sattigeri, R. Feris, R. Giryes, and L. Karlinsky, "Tafssl: Task-adaptive feature sub-space learning for few-shot classification," in *European Conference on Computer Vision*. Springer, 2020, pp. 522–539.
- [32] S. M. Kye, H. B. Lee, H. Kim, and S. J. Hwang, "Transductive few-shot learning with meta-learned confidence," *arXiv preprint arXiv:2002.12017*, 2020.
- [33] C. Simon, P. Koniusz, R. Nock, and M. Harandi, "Adaptive subspaces for few-shot learning," in *Proceedings of the IEEE/CVF Conference on Computer Vision and Pattern Recognition*, 2020, pp. 4136–4145.
- [34] H. Zhang and Q. Yao, "Decoupling representation and classifier for noisy label learning," *arXiv preprint arXiv:2011.08145*, 2020.
- [35] D. Arpit, S. Jastrzebski, N. Ballas, D. Krueger, E. Bengio, M. S. Kanwal, T. Maharaj, A. Fischer, A. Courville, Y. Bengio *et al.*, "A closer look at memorization in deep networks," in *International Conference on Machine Learning*. PMLR, 2017, pp. 233–242.
- [36] Y. Wang, G. Huang, S. Song, X. Pan, Y. Xia, and C. Wu, "Regularizing deep networks with semantic data augmentation," *arXiv preprint arXiv:2007.10538*, 2020.
- [37] C. Shorten and T. M. Khoshgoftaar, "A survey on image data augmentation for deep learning," *Journal of Big Data*, vol. 6, no. 1, p. 60, 2019.
- [38] Y. LeCun, L. Bottou, Y. Bengio, and P. Haffner, "Gradient-based learning applied to document recognition," *Proceedings of the IEEE*, vol. 86, no. 11, pp. 2278–2324, 1998.
- [39] M. C. Shin, K. I. Chang, and L. V. Tsap, "Does colorspace transformation make any difference on skin detection?" in *Sixth IEEE Workshop on Applications of Computer Vision, 2002.(WACV 2002). Proceedings*. IEEE, 2002, pp. 275–279.
- [40] F. J. Moreno-Barea, F. Strazzera, J. M. Jerez, D. Urda, and L. Franco, "Forward noise adjustment scheme for data augmentation," in *2018 IEEE Symposium Series on Computational Intelligence (SSCI)*. IEEE, 2018, pp. 728–734.
- [41] A. Antoniou, A. Storkey, and H. Edwards, "Data augmentation generative adversarial networks," *arXiv preprint arXiv:1711.04340*, 2017.
- [42] X. Zheng, T. Chalasani, K. Ghosal, S. Lutz, and A. Smolic, "Stada: Style transfer as data augmentation," *arXiv preprint arXiv:1909.01056*, 2019.
- [43] H. Inoue, "Data augmentation by pairing samples for images classification," *arXiv preprint arXiv:1801.02929*, 2018.

- [44] T. DeVries and G. W. Taylor, "Dataset augmentation in feature space," *arXiv preprint arXiv:1702.05538*, 2017.
- [45] C. Bowles, L. Chen, R. Guerrero, P. Bentley, R. Gunn, A. Hammers, D. A. Dickie, M. V. Hernández, J. Wardlaw, and D. Rueckert, "Gan augmentation: Augmenting training data using generative adversarial networks," *arXiv preprint arXiv:1810.10863*, 2018.
- [46] Y. Bengio, A. Courville, and P. Vincent, "Representation learning: A review and new perspectives," *IEEE transactions on pattern analysis and machine intelligence*, vol. 35, no. 8, pp. 1798–1828, 2013.
- [47] M. F. Mathieu, J. J. Zhao, J. Zhao, A. Ramesh, P. Sprechmann, and Y. LeCun, "Disentangling factors of variation in deep representation using adversarial training," in *Advances in neural information processing systems*, 2016, pp. 5040–5048.
- [48] A. H. Jha, S. Anand, M. Singh, and V. Veeravasaru, "Disentangling factors of variation with cycle-consistent variational auto-encoders," in *European Conference on Computer Vision*. Springer, 2018, pp. 829–845.
- [49] D. Bouchacourt, R. Tomioka, and S. Nowozin, "Multi-level variational autoencoder: Learning disentangled representations from grouped observations," *arXiv preprint arXiv:1705.08841*, 2017.
- [50] H. Hosoya, "Group-based learning of disentangled representations with generalizability for novel contents," in *IJCAI*, 2019, pp. 2506–2513.
- [51] J. Nemeth, "Adversarial disentanglement with grouped observations," *arXiv preprint arXiv:2001.04761*, 2020.
- [52] L. Fei-Fei, R. Fergus, and P. Perona, "One-shot learning of object categories," *TPAMI*, vol. 28, no. 4, pp. 594–611, 2006.
- [53] B. M. Lake, R. Salakhutdinov, and J. B. Tenenbaum, "Human-level concept learning through probabilistic program induction," *Science*, vol. 350, no. 6266, pp. 1332–1338, 2015.
- [54] J. Snell, K. Swersky, and R. Zemel, "Prototypical networks for few-shot learning," in *NIPS*, 2017.
- [55] F. S. Y. Yang, L. Zhang, T. Xiang, P. H. Torr, and T. M. Hospedales, "Learning to compare: Relation network for few-shot learning," in *CVPR*, 2018.
- [56] S. Ravi and H. Larochelle, "Optimization as a model for few-shot learning," in *ICLR*, 2017.
- [57] C. Finn, P. Abbeel, and S. Levine, "Model-agnostic meta-learning for fast adaptation of deep networks," in *ICML*, 2017.
- [58] A. Santoro, S. Bartunov, M. Botvinick, D. Wierstra, and T. Lillicrap, "Meta-learning with memory-augmented neural networks," in *ICML*, 2016.
- [59] N. Mishra, M. Rohaninejad, X. Chen, and P. Abbeel, "A simple neural attentive meta-learner," in *ICLR*, 2018.
- [60] T. Munkhdalai and H. Yu, "Meta networks," in *ICML*, 2017.
- [61] T. Munkhdalai, X. Yuan, S. Mehri, and A. Trischler, "Rapid adaptation with conditionally shifted neurons," in *ICML*, 2018.
- [62] S. Gidaris and N. Komodakis, "Dynamic few-shot visual learning without forgetting," in *CVPR*, 2018.
- [63] S. Qiao, C. Liu, W. Shen, and A. L. Yuille, "Few-shot image recognition by predicting parameters from activations," in *CVPR*, 2018.



Haipeng Zhang received the B.S. degree from the Department of Physics, Tsinghua University, Beijing, China, in 2016, and he is currently working toward the Ph.D. degree in the Department of Automation, Tsinghua University, Beijing, China.

His research interests include machine learning, deep learning and computer vision.



Zhong Cao received the B.S. degree from the Department of Automation, Tsinghua University, Beijing, China, in 2014, and he is currently working toward the Ph.D. degree in the Department of Automation, Tsinghua University, Beijing, China.

His research interests include machine learning, deep learning and computer vision.



Ziang Yan received the B.S. degree from the Department of Automation, Tsinghua University, Beijing, China, in 2015, and he is currently working toward the Ph.D. degree in the Department of Automation, Tsinghua University, Beijing, China.

His research interests include machine learning, deep learning and computer vision.



Changshui Zhang (M'02–SM'15–F'18) received the B.S. degree in mathematics from Peking University, Beijing, China, in 1986, and the M.S. and Ph.D. degrees in control science and engineering from Tsinghua University, Beijing, in 1989 and 1992, respectively.

He is currently a Professor with the Department of Automation, Tsinghua University. His research interests include artificial intelligence, image processing and machine learning.